Low-dose cadmium potentiates lung inflammatory response to 2009 pandemic H1N1 influenza virus in mice

Joshua D. Chandler[*], Xin Hu[*], Eunju Ko[†], Soojin Park[†], Jolyn Fernandes[*], Young-Tae Lee[†], Michael L. Orr[*], Li Hao[*], M. Ryan Smith[*], David C. Neujahr[*], Karan Uppal[*], Sang-Moo Kang[†], Dean P. Jones[*‡] and Young-Mi Go[*‡]

[*] Division of Pulmonary, Allergy and Critical Care Medicine, Emory University School of Medicine, Atlanta, GA, 30322, [†] Center for Inflammation, Immunity and Infection, Georgia State University, Atlanta, GA, 30303.

Running Head: Cadmium potentiates H1N1 lung inflammation in mice

[‡] Corresponding authors: Whitehead Biomedical Research Building, 615 Michael St, Room 225 Atlanta, GA, 30322. Phone: 404-727-5984. Fax: 404-727-2974. E-mail: ygo@emory.edu, dpjones@emory.edu

Abbreviations

Cd, Cadmium; Ctl, control; Cys, cysteine; CySS, cystine; FACS, fluorescence-activated cell sorting; FDR, False discovery rate; GSEA, Gene set enrichment analysis; H1N1, pandemic 2009 influenza A (H1N1) virus; HRM, High resolution metabolomics; ICP-MS, Inductively coupled plasma mass spectrometer; interferon gamma, IFN-γ; interleukin-1beta, IL-1β; LC, liquid chromatograph; MS, mass spectrometer; *m/z*, mass to charge; RT, retention time; sPLS, sparse partial least squares; Trx, thioredoxin.

Abstract

Cadmium (Cd) is a toxic, pro-inflammatory metal ubiquitous in the diet that accumulates in body organs due to inefficient elimination. Responses to influenza virus infection are variable, particularly severity of pneumonia. We used a murine model of chronic low-dose oral exposure to Cd to test if increased lung tissue Cd worsened inflammation in response to sub-lethal H1N1 infection. Using histopathology and flow cytometry, we observed increased lung inflammation in Cd-treated mice given H1N1 compared to H1N1 alone, including neutrophils, monocytes, T lymphocytes and dendritic cells. Lung genetic responses to infection (increasing TNF-α, interferon and complement, and decreasing myogenesis) were also exacerbated. To reveal the organization of a network structure, pinpointing molecules critical to Cd-altered lung function, global correlations were made for immune cell counts, leading edge gene transcripts and metabolites. This revealed that Cd increased correlation of myeloid immune cells with pro-inflammatory genes, particularly interferon-γ and metabolites. Together, the results show that Cd burden in mice increased inflammation in response to sub-lethal H1N1 challenge, which was coordinated by genetic and metabolic responses, and could provide new targets for intervention against lethal inflammatory pathology of clinical H1N1 infection.

Keywords: Environmental safety, exposome, heavy metals, influenza A virus, public health.

Introduction

Recent studies of the environmental toxic metal cadmium (Cd) show that Cd at levels found in human lungs potentiates pro-inflammatory signaling by the redox-sensitive transcription factor NF-κB (1, 2). Cd is a commercially important metal used in NiCd batteries, plating, pigments and plastics (3-5). Earlier occupational toxicities from Cd have been largely eliminated by occupational hygiene, and tobacco use remains as a major avoidable source of exposure. In non-smokers, diet is the most important source of human Cd burden, on average representing about half of the exposure of individuals with active tobacco use (6, 7). Although Cd is poorly absorbed, there is no effective mechanism for elimination so that the biological half-life in humans is over 10 years (7, 8). Our mechanistic studies show that low concentrations of Cd cause oxidation of thiol/disulfide redox systems (9-11), disrupt the actin-cytoskeleton regulation (10), cause translocation of thioredoxin-1 (Trx1) into the nucleus (10), increase NF-κB activity and increase pro-inflammatory cytokines (9, 12). Cd causes a dose-dependent oxidation of plasma cysteine/cystine (Cys/CySS) redox state (E_h CySS, Y.-M. Go, unpublished), the major low molecular weight thiol/disulfide system in plasma previously associated with pro-inflammatory signaling (13, 14). Additionally, studies with a transgenic NLS-thioredoxin-1 (Trx1) mouse showed that increased nuclear Trx1 substantially potentiated adverse outcome from H1N1 influenza infection (9) and also increased oxidation of thiol/disulfide redox systems (9).

H1N1 and other influenza A strains are highly infectious (15, 16) and cause variable severity of disease (17-22). Viral factors affecting virulence are well known, but these do not account for inter-individual variations in host responses. Host genetics impact severity of response (23, 24), but inter-individual differences in sensitivity have mainly been linked to

demographic factors, such as age and general health (25, 26). In most cases, the pandemic 2009 influenza A (H1N1) virus caused an uncomplicated respiratory tract illness with symptoms similar to those caused by seasonal influenza viruses. However, severe responses also occurred in a small fraction of patients and were linked biologically to high production of pro-inflammatory cytokines termed a "cytokine storm" (27, 28) as well as to excess activity of the complement system (29). The cytokine storm included high levels of IL-6 and was strongly associated with decreased lung function and death (30, 31).

The current study was designed to test whether Cd burden, at a level found in lungs of non-smokers, enhanced severity of HIN1 influenza virus infection in a mouse model. Mice were given water ad libitum without or with $CdCl_2$ (1 mg/L) for 16 weeks, and 10 days before sacrifice each mouse was given sub-lethal H1N1 or mock (sterile saline) by intranasal exposure. Lung histopathology and immune cell counts were used to evaluate intensity of inflammatory response and inflammatory pathology. Gene expression analysis and high-resolution metabolomics were used to explore potential Cd-dependent mechanisms associated with severity of response using the open-source software, xMWAS (32). Targeted analysis of IFN-γ protein correlations with immune cells was used to confirm xMWAS results.

Materials and Methods

Animals

All experimental protocols for animal studies were approved by Emory University and Georgia State University Internal Care and Use Committees. Experimental methods were carried out in accordance with the relevant guidelines and regulations. Male C57BL6 mice (n = 11 - 13 per group) aged 8 weeks (Jackson Labs, Bar Harbor, ME, USA) were maintained in clean facilities and given sterile-filtered drinking water with 1 mg/L $CdCl_2$ (Sigma-Aldrich, St. Louis, MO, USA) or vehicle for 16 weeks. Food content of Cd (62 ± 1 ng/g food) was negligible compared to the Cd derived from water (1). Ten days prior to study completion, mice were inoculated with H1N1 (A/California/04/2009; dose of 0.6×10^3 pfu) under isoflurane anesthesia. Prior to our main study, optimal virus dose was determined to achieve maximal sub-lethal morbidity based on body weight loss and lung histopathology (Supplement 1). Day 10 was chosen as the time point of maximal sub-lethal morbidity but also as a clinically relevant time point for severe and persistent cases. People infected with influenza are generally asymptomatic for 1 - 4 days, then exhibit symptoms for 3 - 7 days (https://www.cdc.gov/flu/professionals/acip/clinical.htm).

For the main study, mice were weighed every 7 days until infection, then daily. Mice were observed daily for other signs of influenza morbidity, e.g., a ruffled hair coat, activity or labored breathing, and no apparent differences were observed between H1N1 and Cd+H1N1. We previously found that low-dose Cd increased airway reactivity as measured by airway enhanced pause (PenH) and used this test to evaluate possible airway effects (33, 34). This test does not require additional drug (e.g., methacholine) treatment which could impact the lung metabolome.

Cd measurement by Inductively-Coupled Plasma Mass Spectrometry (ICP-MS)

Lung tissue ^{114}Cd was assayed as previously described (1). ICP-MS procedures conformed to accuracy (100 ± 10%) and precision standards (relative standard deviation < 12%). Cd values were normalized to tissue mass. Human lung tissue samples were collected in the Emory Transplant Center (Emory IRB protocol 000006248) and maintained frozen at -80 ˚C until analysis.

Flow cytometry and staining

Immune cells in lung tissue were quantified by fluorescence-activated cell sorting (FACS). Lung tissues were homogenized in DMEM and applied to Percoll gradients before washing with PBS. Total viable cells were counted using a hemocytometer with 0.4% trypan blue for dye exclusion. A subset of cells for FACS analysis was treated with anti-surface marker antibodies including CD11b (M1/70), CD45 (30-F11), B220 (RA3-6B2), Siglec F (E50-2440) (BD Pharmingen, Franklin Lakes, NJ, USA); CD11c (N418), F4/80 (BM8) (eBioscience, Thermo Fisher Scientific, Waltham, MA, USA); and CD103 (2E7), Ly6c (HK1.4), MHC-II (M5/114.15.2), CD3 (17A2), CD4 (GK1.5), and CD8 (53-5.8) (BioLegend, San Diego, CA, USA). Data were acquired using an LSR-II/Fortessa (Becton-Dickinson, Franklin Lakes, NJ, USA) and analyzed using FlowJo v. 10.1 (Tree Star, Inc., Ashland, OR, USA). CD11b$^+$ DCs were gated as those with low CD103 expression, and vice-versa; we did not analyze a mixed population (CD11b$^+$/CD103$^+$). Absolute counts were expressed from the percentage from FACS analysis multiplied by viable cell counts obtained with a hemocytometer.

Analysis of glutathione and cysteine in lung tissue

Glutathione and cysteine in lung tissue were analyzed by HPLC with fluorescence detection (35). Protein assay (bicinchonicic acid) was used to standardize the results to intracellular concentrations.

Histopathology

The lung collected at 10 days after challenge was fixed with 10% normal buffered formalin (NBF) in PBS. After fixation NBF tissues were transferred to 70% alcohol and processed to paraffin using a Shandon Excelsior AS (Thermo Fisher Scientific). For Shandon Excelsior AS, a standard program of dehydration was carried out in ethanol 70%, 80%, 90%, 95%, 100%, 100% 1 hour each, followed by xylenes twice and 30 min each. Finally, the tissue was soaked in paraffin 30 min and repeated once and then hold in the second paraffin bath for at last 1 hour. Left lung tissue sections (4 mice per group) were stained with hematoxylin and eosin (H&E) to assess histopathological changes as described (36). Images were acquired by Axiovert 100 (Zeiss, Oberkochen, Germany) at 100 x magnification, and inflammation was blindly scored as previously described (36).

Transcriptomics

20-25 mg of lung tissue was stored in RNAlater (Qiagen, Hilden, Germany) prior to lysis and RNA isolation using the miRNEasy kit (Qiagen, Hilden, Germany). 250 ng of RNA was prepared and hybridized to MoGene ST 2.0 arrays (Affymetrix, Thermo Fisher Scientific, Waltham, MA, USA). CEL files were converted to a Robust-Multi Array (RMA) and loaded in the gene set enrichment analysis (GSEA) Java applet (v. 2.2; Broad Institute) to test gene set

enrichment. Annotations were made using MSigDB file 'MoGene_2_0_st.chip', accessed from the GSEA applet. Redundant annotations were collapsed using maximum intensities.

High resolution metabolomics (HRM)

Lung tissue metabolites were extracted from 20-30 mg tissue in 15 µl/mg of 2:1 acetonitrile:water containing internal standards per mg tissue (33). Tissues were sonicated, vortexed and incubated on ice for 30 minutes before centrifugation at 16,000 g and 4 ˚C. Five µl of supernatant was injected on a Dionex Ultimate 3000 LC system coupled to Thermo QExactive High Field mass spectrometer (Thermo Fisher Scientific, Waltham, MA, USA); each analysis was performed with three technical replicates. Chromatographic separation was achieved with Accucore HILIC (100 x 2.1 mm, 2.6 µm, 80 Å) chromatography (Thermo Fisher Scientific, Waltham, MA, USA). Untargeted data were extracted with XCMS (37) and xMSanalyzer (38), recovering 2,956 features (high resolution *m/z* paired with retention time, normalized and log transformed relative abundance of each metabolic features. Feature intensities were $\log_2$ transformed prior to integrative network analysis using xMWAS (32). *Mummichog* pathway enrichment analysis was used to identify metabolic pathways enriched in mass spectral features obtained from xMWAS analyses (32); this approach was previously validated for relevant metabolites by coelution with pure standards and MS^2 spectra (39, 40).

Data integration and network analysis

Immune cells (Cd+H1N1 significantly different from H1N1 alone), gene transcripts (from leading of gene sets significantly different between Cd+H1N1 and H1N1 alone) and lung *m/z* features (all) were selected for xMWAS analysis to identify biological and molecular

relationships during H1N1 infection. xMWAS (32) uses the sparse partial least squares (sPLS) regression method and the *network()* function implemented in R package mixOmics (41, 42) for generating the association matrices between datasets, with Student's t-test used to evaluate the statistical significance of pairwise association scores.

Statistics

Data are presented as the mean and standard error of the mean. One-way ANOVA with Holm-Sidak's post-test was used to test statistical significance, except for histopathology (Figure 1), which used Student's t-test. The significance level was $p < 0.05$ for all statistical tests, which were two-tailed. The GSEA applet (v. 2.2; Broad Institute) produced all statistics for gene set enrichment (43). Genes were ranked according the "Signal2Noise" statistic with a significance threshold of false discovery rate (FDR)-adjusted $q < 0.05$.

Data Sharing

Metabolomics and GSEA of transcriptomics data have been provided in Supplemental Tables with the manuscript. Other data are available upon reasonable request.

Results

A sub-lethal dose of H1N1 was selected to examine mouse lung inflammation, genetic and metabolic responses to low dose Cd exposure

Selection of H1N1 virus titer for mouse infection is critical for this study to achieve maximal sub-lethal morbidity as evaluated by body mass decrease and increased lung inflammation at Day 10 post-infection. We compared the effects of 5 different virus doses-induced infections on lethality and severity of lung infection measuring body weight and lung inflammation (**Supplemental Fig 1A**). The results showed that the virus dose at 0.6 x 10^3 pfu maximized body weight loss at Day 10 post-infection without increasing lethality. Higher doses increased lethality, and lower doses caused less morbidity resulting in recovery after Day 8. Higher doses also caused maximally detectible histopathological changes (**Supplemental Fig 1B**) which would have prevented detecting second-hit changes by Cd [least lung inflammation at 0.6 x 10^3 pfu compared with top two high doses (1.2 x 10^3 pfu and 0.9 x 10^3 pfu)]. Based on this result, we selected dose of H1N1 virus (0.6 x 10^3 pfu) to infect mice 10 days before completion of the study period. Thus, four groups of mice were maintained for a 16-week treatment period, half receiving water and half receiving low-dose Cd exposure. At 10 days prior to termination, half of each group received vehicle (Control, Cd groups) and half received the H1N1 dose (H1N1, Cd+H1N1).

Cd worsened pathology of H1N1 infection

We examined lung histopathology to determine the extent of inflammation. Histopathological analysis showed that H1N1 infection caused significant inflammation compared to control, and Cd treatment increased the inflammation caused by H1N1 infection [inflammation scores (mean

± SE): H1N1, 288.3 ± 15.3%; Cd+H1N1, 344.2 ± 16.3%, Fig 1]. Cd alone did not have statistically significant effect (Ctl, 100 ± 14.9%; Cd, 109.5 ± 11.5, **Fig. 1**). Mice treated with Cd showed an increase in lung Cd in both Cd and Cd+H1N1 groups (**Supplemental Fig. 1C**). To compare our model to human lung Cd, we used the same analytical methods to measure Cd in available lung samples from smokers (S) and non-smokers (NS) (**Supplemental Fig. 1C**). The results show that Cd content (pmol Cd/g wet tissue, mean ± SE) in Cd-treated mouse lung tissue [Cd (n = 9), 239 ± 27.9; Cd+H1N1 (n = 5), 212 ± 53.0] overlapped the range of non-smokers (n = 5, 156 ± 29.2) and lower portion of the range for smokers (n = 14, 568 ± 137.1). Cd amounts measured in control and H1N1 groups were lower, 74 ± 24.1 (n = 5) and 26 ± 6.1 (n = 9), respectively. Consistent with previous low-dose Cd studies (44), Cd had no effect on body mass or weight gain (**Supplemental Fig. 1D**). Cd also had no effect on weight loss following infection (final weights of weight at inoculation: H1N1, 78 ± 2%; Cd+H1N1, 79 ± 2%, **Supplemental Fig. 1D**).

Cd increased H1N1-mediated lung inflammation

In addition to histopathologic examination of inflammation, we also quantified lung inflammation with measurements of immune cells by flow cytometry (**Fig. 2**). Increased immune cell content in lungs substantially reinforced the histopathology data showing increased inflammation in Cd-exposed mice. Neutrophils, monocytes, $CD11b^+$ dendritic cells (DCs), $CD103^+$ DCs, plasmacytoid DCs (pDCs), $CD4^+$ T lymphocytes and $CD8^+$ T lymphocytes were increased in lungs of Cd+H1N1 compared to H1N1 ($p < 0.05$ each, **Fig. 2A-G**).

Cd enhanced pro-inflammatory gene set expression in H1N1-infected mice

To determine whether Cd impacted gene expression following H1N1 infection, we used Affymetrix MoGene ST 2.0 arrays followed by Gene Set Enrichment Analysis (GSEA) (43) to study effects on transcript abundances among the treatment groups (n = 5). We used GSEA gene sets with FDR $q < 0.05$ for gene set enrichment comparing overrepresentation of gene sets between experimental groups. Seven gene sets were different when comparing Cd+H1N1 and H1N1 (**Table 1**), including six that were overrepresented in Cd+H1N1 compared to H1N1 alone (1. allograft rejection, 2. complement signaling, 3. Inflammatory response, 4. IFN-α response, 5. IFN-γ response, 6. TNF-α signaling via NF-κB; comprised of pro-inflammatory genes). The myogenesis of the seventh gene set was overrepresented in H1N1 compared to Cd+H1N1 (myogenesis; comprised of cytoskeletal subunit-encoding genes, **Table 1**). Each of the six gene sets overrepresented in Cd+H1N1 compared to H1N1 was also overrepresented in either group compared to control or Cd alone. Notably, the myogenesis gene set was overrepresented in all other groups (Ctl, Cd, or H1N1) compared to Cd+H1N1.

The leading edge genes from each of the gene sets in **Table 1** were selected for global correlation analysis by xMWAS (32). After accounting for redundancies across gene sets, this yielded 293 leading edge genes. Two-hundred and twenty of these genes belonged to the pro-inflammatory gene sets in Table 1 that were increased in Cd+H1N1 compared to H1N1. Pro-inflammatory leading edge genes were predominantly comprised of cytokines, chemokines, receptors of cell activation and signaling proteins. The highest ranked leading edge gene from these sets (contributing most to their enrichment) was ‘interleukin 6 (interferon, beta 2)’ (*Il6*). Several of the inflammatory genes in these sets were increased in Cd+H1N1 compared to those in H1N1, including IFN-γ (*Ifng*), IL-1β (*Il1b*), IL-6 (*Il6*), and IP-10 (*Cxcl10*) (average increase of 1.5 ± 0.1-fold comparing Cd+H1N1 to H1N1). The remaining 73 leading edge genes belonged

to the myogenesis gene set with cytoskeletal subunit and regulatory genes including 'actin, alpha 1' (*Acta1*), 'creatine kinase, muscle' (*Ckm*) and 'collagen 1A1' (*Col1a1*). The lowest ranked gene from this gene set (contributing most to "negative enrichment" in Cd+H1N1) was 'myosin, light chain 7, regulatory' (*Myl7*). Unlike the other genes, leading edge genes from the myogenesis gene set were decreased by Cd+H1N1 compared to H1N1.

Global correlation analysis of Cd effect on lung response to H1N1 influenza infection

To reveal organization of the network structure and pinpoint molecules critical to Cd-altered lung function, global correlations were made for immune cell counts, leading edge gene transcripts and metabolites using xMWAS (32). xMWAS is a data-driven integration and network analysis tool which uses community detection to improve understanding of complex interactions. As input, we used inflammatory cells as measured in **Fig. 2A-G**, the 293 leading edge genes, and lung tissue metabolites measured by HRM (total of 2,956 metabolic features) to produce association networks specific to H1N1 and Cd+H1N1 experimental groups (**Fig. 3**; n = 5). Student's t-test was used to determine the association score (absolute value) threshold of 0.88 at $p < 0.05$ and n = 5.

The resulting networks of H1N1 was comprised of 426 metabolic features, 160 gene transcripts and 7 immune cells types, while the networks of Cd+H1N1 was comprised of 478 metabolic features, 158 gene transcripts and 6 immune cell types (**Fig. 3A**; full network membership given in **Supplemental Table 1**).

The visualized correlations between molecules (metabolites, transcripts, immune cells) use the absolute change in eigenvector centrality, calculated by xMWAS, to quantify centrality (**Fig. 3B**), where centrality is a measure of relative network importance. The results showed that

all immune cells (blue triangles) except for neutrophils (indicated by PMN, **Fig. 3A left**) were closely clustered together in the H1N1 network, reflecting many overlapping correlations across gene transcripts and metabolic features involved in inflammation for this experimental group. By contrast, in the Cd+H1N1 network, monocytes, $CD11b^+$ DCs and neutrophils were clustered tightly together, while T lymphocytes and pDCs were more de-centralized (**Fig. 3A** right). Respective delta centrality scores showed that monocytes (+0.419), $CD11b^+$ DCs (+0.380) and neutrophils (+0.301) had increased centrality in the Cd+H1N1 network compared to H1N1 (**Fig. 3B**). Additionally, $CD103^+$, a lymphoid dendritic cell sub-population, was not found in the Cd+H1N1 network (**Fig. 3A right**). Thus, H1N1 resulted in clustering containing myeloid and lymphoid cell populations, but Cd+H1N1 resulted in clustering with only myeloid cell types.

Previous research showed that influenza-induced IFN-γ restricts protective innate lymphoid cell group II function in mouse lung following challenge with H1N1 (45). We therefore performed targeted tests to determine whether correlations with IFN-γ differed for myeloid and lymphoid cells in Cd+H1N1 compared to H1N1. Results showed that each myeloid cell count correlated with IFN-γ only in Cd+H1N1 mice [*monocytes* (Cd+H1N1, $r = 0.97$, $p = 3\text{x}10^{-7}$; H1N1, $r = 0.21$, $p = 0.21$; **Fig. 3C**), *$CD11b^+$ DCs* (Cd+H1N1, $r = 0.92$, $p = 2\text{x}10^{-5}$; H1N1, $r = -0.05$, $p = 0.86$; **Fig. 3D**) and *neutrophils* (Cd+H1N1, $r = 0.89$, $p = 9\text{x}10^{-5}$; H1N1, $r = 0.22$, $p = 0.48$; **Fig. 3E**)]. In contrast, significant correlations with IFN-γ did not occur for lymphoid cells in either group (data not shown). The results confirm the global correlation network analysis showing that Cd burden increases centrality of myeloid cells with pro-inflammatory pathways following H1N1 infection and implicate IFN-γ signaling as a potential mechanism.

Gene sets and metabolic pathways associated with Cd effect on immune cell responses to H1N1

We further examined the molecular composition of each of the correlation networks to determine which transcripts and metabolic pathways were central in each group. The overall network composition of Cd+H1N1 and H1N1 overlapped by >50% in both leading edge genes and metabolic features so we improved focus on the most divergent relationships between Cd+H1N1 and H1N1 by analyzing genes and metabolites with delta eigenvector centrality (absolute value), $|\text{Centrality}_{\text{Cd+H1N1}} - \text{Centrality}_{\text{H1N1}}|, \geq 0.1$ for monocytes, $CD11b^{+}$ DCs and neutrophils (**Fig. 3B**). If a gene or metabolic feature was not present in one of the correlation networks, its eigenvector centrality was considered 0 (**Supplemental Table 1**). Results for the transcriptome data showed 83 leading edge genes (**Supplemental Table 2**) were present in the Cd+H1N1 and H1N1 networks, with the IFN-γ response gene set (27.4% of total gene counts; **Fig. 4A and Supplemental Table 2**) being most represented. IFN-α response (17.8%) followed, and myogenesis was least represented (5.2%). The IFN-γ transcript, *Ifng* had differential centrality of +0.435 for Cd+H1N1 network compared to H1N1. The transcript with most positive change for gene centrality (1.0) was immediate early response 2, *Ier2*, encoding a DNA-binding protein, and the transcript with most negative change for gene centrality (-0.88) was Dnaj (Hsp40) homolog, subfamily B, member 4, *DnajB4*, a chaperone protein targeted to the plasma membrane; additional details are provided in **Supplemental Tables 1 and 2**. Thus, the transcript data are consistent with Cd effects occurring through IFN-γ-dependent signaling mechanisms and also involving more complex interactions of nuclear as well as plasma membrane systems.

Prior research has shown that low-dose Cd also has widespread effects on metabolism, with especially related to oxidative stress, mitochondrial β-oxidation of fatty acids and amino

acid metabolism (46). To focus on network centrality among metabolites, we analyzed 165 metabolic features with delta eigenvector centrality ≥0.1, using the metabolic pathway analysis software, *mummichog* 1.0.10 (47). The top pathway was for methionine and cysteine metabolism (**Fig. 4B**), potentially linked to oxidative stress responses. The largest positive centrality change was for S-adenosylhomocysteine (+0.415), an intermediate in methylation processes linked to methionine. Other pathways included vitamin B3 (niacin/NAD), urea cycle and glycerophospholipid metabolism, all of which are connected to mitochondrial function and known to be perturbed by Cd. Other metabolic pathways included amino acid, pyrimidine and purine pathways that have previously been associated with inflammation and/or cell proliferation and turnover (**Fig. 4B**). Consistent with this, the metabolite with the most negative centrality change was adenine (-0.953). The results are consistent with Cd potentiation of inflammation to H1N1 infection through widespread effects of low Cd exposure on oxidative stress, mitochondrial function and regulation of immune cell populations through IFN-γ.

Discussion

A previous study showed that blood concentrations of toxic metals including Cd were significantly higher in H1N1 cases with pneumonia versus pneumonia not caused by H1N1, and two H1N1 cases having highest Cd concentrations did not recover from illness (48). Although limited by the small number of cases, the study suggested that Cd could be a risk factor for inflammatory response and enhanced severity of H1N1 virus infection-induced respiratory diseases. In the present study using a mouse model of H1N1 infection, we show that lung Cd burden, at a value present in human lung, exacerbated inflammation and lung injury from H1N1 infection in mice. Comparing Cd+H1N1 to H1N1-infected mice, Cd increased the day 10 post-infection lung burden of myeloid (monocytes, neutrophils), lymphoid ($CD4^+$ and $CD8^+$ T cells) and multi-origin (DCs) bone marrow lineages of immune cells. Integrated network analysis of omics data further showed that Cd burden shifted the immune response from one centered on both lineages to one with myeloid cells (including $CD11b^+$ DCs) as a dominant central hub. Thus, high Cd burden appears to contribute to worse outcome following H1N1 infection by increasing the immune response with suppression of lymphoid and enhancement of myeloid cell participation in response to infection.

The global correlation network analysis of immune cells with gene transcript and metabolite abundances revealed the centrality of myeloid cells (monocytes, $CD11b^+$ DCs (considered a myeloid DC subtype, (49)) and neutrophils) in the Cd+H1N1 group. Transcriptional responses suggest that Cd primes myeloid cells for tight coordination with IFNγ signaling. The finding that a unique lysosomal thiol reductase, gamma-interferon (IFN-γ)-inducible lysosomal thiol reductase controls conditions for degradation of proteins to small peptides in lysosomes (50, 51), raises the possibility that Cd specifically impacts IFNγ-dependent

functions through interaction with, or oxidation of, the thioredoxin-like active site involved in disulfide reduction. Low dose Cd causes oxidation and disruption of the actin-cytoskeleton (10), suggesting that targeted effects on a critical signaling system could occur even without effects on major GSH or thioredoxin systems. Effects of low-dose Cd on the actin-cytoskeleton system triggers translocation of Trx1 to cell nuclei (10) and increase NF-κB activation (9, 12) and monocyte adhesion (13). Thus, these processes also could contribute to higher immune cell counts in Cd+H1N1 compared to H1N1. The GSEA results showing effects of Cd on pro-inflammatory gene sets (**Table 1**), as well as increased cytokine levels and immune cell counts, support such a Cd-dependent mechanism.

Alternative mechanisms for Cd effects on inflammatory pathology of H1N1 could involve cytoskeletal functions, myogenesis and elastogenesis in the inflamed and injured lungs. It is noteworthy that the combination of Cd pre-treatment with H1N1 infection was the experimental condition to cause a significant negative enrichment, or decrease in overall transcript levels, of the myogenesis gene set. Cytoskeletal regulation by tight junctions and adherens junctions is a key element of airway permeability to infiltrating immune cells (52). We previously found that low dose Cd disruption of actin cytoskeleton regulation (10, 53) triggered nuclear translocation of thioredoxin-1 and caused cell death (12). A study by Desouza *et al*. also showed that actin-binding proteins contribute to cell death, and actin dynamics plays a key role in regulating apoptosis signaling (54). Studies of low dose Cd effects on actin cytoskeleton and cell death in fibroblasts, HeLa and HT-29 cells [(10, 53); Y.-M. Go, D.P. Jones, unpublished] suggest that this could be a general cell response and contribute to barrier dysfunction. Thus, Cd could also contribute to severity of response through mechanisms involving impaired

myogenesis, elastogenesis, increased cell death and failure to clear cell debris in the inflamed and injured lungs.

In contrast to the coherent picture provided by Cd effects on proinflammatory signaling, immune cell accumulation in the lungs and amplified effects on myeloid compared to lymphoid cells, metabolic effects associated with Cd effects were diverse and complex; the results suggested more of a generalized adaptive response than a causal role in exacerbation of inflammation. The top pathway from pathway enrichment analysis was for sulfur-containing amino acids which serve to support GSH synthesis and antioxidant activities. This would appear to be a protective mechanism, but maladaptive effects could also occur at specific subcellular sites. Pathway enrichment analysis also showed that pathways of several amino acids, nucleosides and phospholipids were overrepresented in the networks with differential eigenvector centrality ≥ 0.1 (**Fig. 4B**). Overall, these results suggest that Cd burden causes a complex array of metabolic responses.

Inhaled Cd causes acute pneumonitis and lung edema (55), and intraperitoneal injection of Cd causes lung inflammation in rats (3). However, chronic ingestion of Cd at levels mimicking those derived from the human diet has not previously been directly linked to inflammatory lung disease. The present research with 16 weeks of Cd in drinking water showed little evidence for inflammation without the second stimulus of H1N1 infection. Thus, Cd accumulation with advanced age (> 65 y), tobacco use, metabolic syndrome and/or obesity, may create a sub-clinical state poised to over-react to influenza virus infection-induced inflammation, which may in turn lead to worse morbidity or mortality (56-60). For future research, the dose of virus used in our study permits recovery to study later complications such as fibrosis caused by low-dose Cd (53).

Finally, in light of common consumption of foods with relatively high Cd content (potatoes, cereals), the results indicate that studies in humans are needed to evaluate whether Cd burden is associated with severity of response to influenza infection. Cd burden can be readily evaluated by determination of Cd/creatinine level in urine (61, 62). While there are no approved strategies to prevent Cd accumulation or decrease its burden, mechanisms discussed above could be targeted to prevent Cd-dependent potentiation of influenza severity. For instance, the mechanism for nuclear Trx1 translocation could be targeted to block excessive activation of transcriptional responses. Alternatively, Txnip, a vitamin D_3 binding protein that controls nuclear Trx1 activity (63, 64), could provide a target for therapeutic manipulation. Trp14 catalyzes reduction of cystine (oxidized form of cysteine) (65) and could provide a target to protect against oxidation of proteins and downstream signaling and recruitment of immune cells. Cd also interacts with trace elements including selenium, zinc and iron (6, 66), providing additional strategies for supplement use (48, 56).

In summary, this study showed that mice given Cd at a level achieved in humans from dietary intake had worse lung inflammation and inflammatory pathology after H1N1 influenza infection, in association with enhanced myeloid-dominant pro-inflammatory gene and metabolic responses. Studies are needed to evaluate whether Cd burden contributes to influenza severity in humans. Combined analyses of phenotypic measures with transcriptome and metabolome analyses enable global surveillance of complex systems responses to identify candidate mechanisms and potential therapeutic targets.

Supplemental Figure 1. Data for sub-lethal virus dose selection based on body mass and histopathology, lung Cd content, body mass, PenH and virus titer.

Supplemental Figure 2. Flow cytometry-quantified eosinophils and alveolar macrophages.

Supplemental Table 1. Full correlation network membership of Fig. 3A.

Supplemental Table 2. A table including 83 leading edge genes (eigenvector centrality ≥0.1).

Acknowledgements

Dr. Young-Mi Go and Dr. Dean P. Jones share equal senior authorship in this collaborative research. We thank the Emory Integrated Genomics Core, Dana B. Barr PhD and Priya E. D'Souza MPH for technical assistance.

Funding

This study was supported by NIEHS Grant R01 ES023485 (DPJ and YMG), R21 ES025632 (DPJ and YMG), NIH S10 OD018006 (DPJ), NIH/NIAID grants R01 AI105170 (SMK), R01 AI093772 (SMK), and R21 AI119366 (SMK), and NHLBI F32 1F32HL132493 (JDC) and Cystic Fibrosis Foundation CHANDL16F0 (JDC).

Author Contributions

- Designed research – YMG, DPJ, SMK
- Performed research – JDC, JF, XH, YTL, EJK, SJP, DCN, MRS, MLO, LH
- Contributed new reagents or analytic tools - KU
- Analyzed data – JDC, YTL, SJP, EJK, JF, XH, MRS
- Wrote the paper – JDC, YMG, DPJ

References

1. Chandler, J. D., Wongtrakool, C., Banton, S. A., Li, S., Orr, M. L., Barr, D. B., Neujahr, D. C., Sutliff, R. L., Go, Y. M., and Jones, D. P. (2016) Low-dose oral cadmium increases airway reactivity and lung neuronal gene expression in mice. *Physiol Rep* **4**
2. Olszowski, T., Baranowska-Bosiacka, I., Gutowska, I., and Chlubek, D. (2012) Pro-inflammatory properties of cadmium. *Acta Biochim Pol* **59**, 475-482
3. Kataranovski, M., Mirkov, I., Belij, S., Nikolic, M., Zolotarevski, L., Ciric, D., and Kataranovski, D. (2009) Lungs: remote inflammatory target of systemic cadmium administration in rats. *Environ Toxicol Pharmacol* **28**, 225-231
4. Waalkes, M. P. (2003) Cadmium carcinogenesis. *Mutat Res* **533**, 107-120
5. Zhang, W., Zhi, J., Cui, Y., Zhang, F., Habyarimana, A., Cambier, C., and Gustin, P. (2014) Potentiated interaction between ineffective doses of budesonide and formoterol to control the inhaled cadmium-induced up-regulation of metalloproteinases and acute pulmonary inflammation in rats. *PLoS One* **9**, e109136
6. Riederer, A. M., Belova, A., George, B. J., and Anastas, P. T. (2013) Urinary cadmium in the 1999-2008 U.S. National Health and Nutrition Examination Survey (NHANES). *Environ Sci Technol* **47**, 1137-1147
7. Satarug, S., and Moore, M. R. (2004) Adverse health effects of chronic exposure to low-level cadmium in foodstuffs and cigarette smoke. *Environ Health Perspect* **112**, 1099-1103
8. Suwazono, Y., Kido, T., Nakagawa, H., Nishijo, M., Honda, R., Kobayashi, E., Dochi, M., and Nogawa, K. (2009) Biological half-life of cadmium in the urine of inhabitants after cessation of cadmium exposure. *Biomarkers* **14**, 77-81
9. Go, Y. M., Kang, S. M., Roede, J. R., Orr, M., and Jones, D. P. (2011) Increased inflammatory signaling and lethality of influenza H1N1 by nuclear thioredoxin-1. *PLoS One* **6**, e18918
10. Go, Y. M., Orr, M., and Jones, D. P. (2013) Actin cytoskeleton redox proteome oxidation by cadmium. *Am J Physiol Lung Cell Mol Physiol* **305**, L831-843
11. Go, Y. M., Roede, J. R., Orr, M., Liang, Y., and Jones, D. P. (2014) Integrated redox proteomics and metabolomics of mitochondria to identify mechanisms of cd toxicity. *Toxicological sciences* **139**, 59-73

12. Go, Y. M., Orr, M., and Jones, D. P. (2013) Increased nuclear thioredoxin-1 potentiates cadmium-induced cytotoxicity. *Toxicological sciences* **131**, 84-94
13. Go, Y. M., and Jones, D. P. (2005) Intracellular proatherogenic events and cell adhesion modulated by extracellular thiol/disulfide redox state. *Circulation* **111**, 2973-2980
14. Go, Y. M., and Jones, D. P. (2011) Cysteine/cystine redox signaling in cardiovascular disease. *Free Radic Biol Med* **50**, 495-509
15. Liu, M., Zhao, X., Hua, S., Du, X., Peng, Y., Li, X., Lan, Y., Wang, D., Wu, A., Shu, Y., and Jiang, T. (2015) Antigenic Patterns and Evolution of the Human Influenza A (H1N1) Virus. *Sci Rep* **5**, 14171
16. Xing, Z. H., Sun, X., Xu, L., Wu, Q., Li, L., Wu, X. J., Shao, X. G., Zhao, X. Q., Wang, J. H., Ma, L. Y., and Wang, K. (2015) Thin-section computed tomography detects long-term pulmonary sequelae 3 years after novel influenza A virus-associated pneumonia. *Chin Med J (Engl)* **128**, 902-908
17. Safronetz, D., Rockx, B., Feldmann, F., Belisle, S. E., Palermo, R. E., Brining, D., Gardner, D., Proll, S. C., Marzi, A., Tsuda, Y., Lacasse, R. A., Kercher, L., York, A., Korth, M. J., Long, D., Rosenke, R., Shupert, W. L., Aranda, C. A., Mattoon, J. S., Kobasa, D., Kobinger, G., Li, Y., Taubenberger, J. K., Richt, J. A., Parnell, M., Ebihara, H., Kawaoka, Y., Katze, M. G., and Feldmann, H. (2011) Pandemic swine-origin H1N1 influenza A virus isolates show heterogeneous virulence in macaques. *J Virol* **85**, 1214-1223
18. Baigent, S. J., and McCauley, J. W. (2003) Influenza type A in humans, mammals and birds: determinants of virus virulence, host-range and interspecies transmission. *Bioessays* **25**, 657-671
19. Taubenberger, J. K., and Kash, J. C. (2010) Influenza virus evolution, host adaptation, and pandemic formation. *Cell Host Microbe* **7**, 440-451
20. Baigent, S. J., and McCauley, J. W. (2003) Influenza type A in humans, mammals and birds: determinants of virus virulence, host-range and interspecies transmission. *Bioessays* **25**, 657-671
21. Safronetz, D., Rockx, B., Feldmann, F., Belisle, S. E., Palermo, R. E., Brining, D., Gardner, D., Proll, S. C., Marzi, A., Tsuda, Y., Lacasse, R. A., Kercher, L., York, A., Korth, M. J., Long, D., Rosenke, R., Shupert, W. L., Aranda, C. A., Mattoon, J. S.,

Kobasa, D., Kobinger, G., Li, Y., Taubenberger, J. K., Richt, J. A., Parnell, M., Ebihara, H., Kawaoka, Y., Katze, M. G., and Feldmann, H. (2011) Pandemic swine-origin H1N1 influenza A virus isolates show heterogeneous virulence in macaques. *J Virol* **85**, 1214-1223

22. Taubenberger, J. K., and Kash, J. C. (2010) Influenza virus evolution, host adaptation, and pandemic formation. *Cell Host Microbe* **7**, 440-451
23. Horby, P., Nguyen, N. Y., Dunstan, S. J., and Baillie, J. K. (2012) The role of host genetics in susceptibility to influenza: a systematic review. *PLoS One* **7**, e33180
24. Horby, P., Nguyen, N. Y., Dunstan, S. J., and Baillie, J. K. (2013) An updated systematic review of the role of host genetics in susceptibility to influenza. *Influenza Other Respir Viruses* **7 Suppl 2**, 37-41
25. Gagnon, A., Miller, M. S., Hallman, S. A., Bourbeau, R., Herring, D. A., Earn, D. J., and Madrenas, J. (2013) Age-specific mortality during the 1918 influenza pandemic: unravelling the mystery of high young adult mortality. *PLoS One* **8**, e69586
26. Wilson, N., Oliver, J., Rice, G., Summers, J. A., Baker, M. G., Waller, M., and Shanks, G. D. (2014) Age-specific mortality during the 1918-19 influenza pandemic and possible relationship to the 1889-92 influenza pandemic. *J Infect Dis* **210**, 993-995
27. Gautam, M. (2012) Endothelial cells as regulators of cytokine storms during influenza infection. *Thorax* **67**, 617-617
28. Liu, Q., Zhou, Y. H., and Yang, Z. Q. (2016) The cytokine storm of severe influenza and development of immunomodulatory therapy. *Cell Mol Immunol* **13**, 3-10
29. Monsalvo, A. C., Batalle, J. P., Lopez, M. F., Krause, J. C., Klemenc, J., Hernandez, J. Z., Maskin, B., Bugna, J., Rubinstein, C., Aguilar, L., Dalurzo, L., Libster, R., Savy, V., Baumeister, E., Cabral, G., Font, J., Solari, L., Weller, K. P., Johnson, J., Echavarria, M., Edwards, K. M., Chappell, J. D., Crowe, J. E., Jr., Williams, J. V., Melendi, G. A., and Polack, F. P. (2011) Severe pandemic 2009 H1N1 influenza disease due to pathogenic immune complexes. *Nat Med* **17**, 195-199
30. Bermejo-Martin, J. F., Ortiz de Lejarazu, R., Pumarola, T., Rello, J., Almansa, R., Ramirez, P., Martin-Loeches, I., Varillas, D., Gallegos, M. C., Seron, C., Micheloud, D., Gomez, J. M., Tenorio-Abreu, A., Ramos, M. J., Molina, M. L., Huidobro, S., Sanchez, E., Gordon, M., Fernandez, V., Del Castillo, A., Marcos, M. A., Villanueva, B., Lopez,

C. J., Rodriguez-Dominguez, M., Galan, J. C., Canton, R., Lietor, A., Rojo, S., Eiros, J. M., Hinojosa, C., Gonzalez, I., Torner, N., Banner, D., Leon, A., Cuesta, P., Rowe, T., and Kelvin, D. J. (2009) Th1 and Th17 hypercytokinemia as early host response signature in severe pandemic influenza. *Crit Care* **13**, R201

31. To, K. K., Hung, I. F., Li, I. W., Lee, K. L., Koo, C. K., Yan, W. W., Liu, R., Ho, K. Y., Chu, K. H., Watt, C. L., Luk, W. K., Lai, K. Y., Chow, F. L., Mok, T., Buckley, T., Chan, J. F., Wong, S. S., Zheng, B., Chen, H., Lau, C. C., Tse, H., Cheng, V. C., Chan, K. H., and Yuen, K. Y. (2010) Delayed clearance of viral load and marked cytokine activation in severe cases of pandemic H1N1 2009 influenza virus infection. *Clin Infect Dis* **50**, 850-859
32. Uppal, K., Ma, C., Go, Y. M., Jones, D. P., and Wren, J. (2018) xMWAS: a data-driven integration and differential network analysis tool. *Bioinformatics* **34**, 701-702
33. Chandler, J. D., Hu, X., Ko, E. J., Park, S., Lee, Y. T., Orr, M., Fernandes, J., Uppal, K., Kang, S. M., Jones, D. P., and Go, Y. M. (2016) Metabolic pathways of lung inflammation revealed by high-resolution metabolomics (HRM) of H1N1 influenza virus infection in mice. *Am J Physiol Regul Integr Comp Physiol* **311**, R906-R916
34. Hwang, H. S., Lee, Y. T., Kim, K. H., Park, S., Kwon, Y. M., Lee, Y., Ko, E. J., Jung, Y. J., Lee, J. S., Kim, Y. J., Lee, Y. N., Kim, M. C., Cho, M., and Kang, S. M. (2016) Combined virus-like particle and fusion protein-encoding DNA vaccination of cotton rats induces protection against respiratory syncytial virus without causing vaccine-enhanced disease. *Virology* **494**, 215-224
35. Jones, D. P., and Liang, Y. (2009) Measuring the poise of thiol/disulfide couples in vivo. *Free Radic Biol Med* **47**, 1329-1338
36. Ko, E. J., Lee, Y. T., Kim, K. H., Jung, Y. J., Lee, Y., Denning, T. L., and Kang, S. M. (2016) Effects of MF59 Adjuvant on Induction of Isotype-Switched IgG Antibodies and Protection after Immunization with T-Dependent Influenza Virus Vaccine in the Absence of CD4+ T Cells. *J Virol* **90**, 6976-6988
37. Smith, C. A., Want, E. J., O'Maille, G., Abagyan, R., and Siuzdak, G. (2006) XCMS: processing mass spectrometry data for metabolite profiling using nonlinear peak alignment, matching, and identification. *Anal Chem* **78**, 779-787

38. Uppal, K., Soltow, Q. A., Strobel, F. H., Pittard, W. S., Gernert, K. M., Yu, T., and Jones, D. P. (2013) xMSanalyzer: automated pipeline for improved feature detection and downstream analysis of large-scale, non-targeted metabolomics data. *BMC Bioinformatics* **14**, 15

39. Frediani, J. K., Jones, D. P., Tukvadze, N., Uppal, K., Sanikidze, E., Kipiani, M., Tran, V. T., Hebbar, G., Walker, D. I., Kempker, R. R., Kurani, S. S., Colas, R. A., Dalli, J., Tangpricha, V., Serhan, C. N., Blumberg, H. M., and Ziegler, T. R. (2014) Plasma metabolomics in human pulmonary tuberculosis disease: a pilot study. *PLoS One* **9**, e108854

40. Uppal, K., Walker, D. I., and Jones, D. P. (2017) xMSannotator: An R Package for Network-Based Annotation of High-Resolution Metabolomics Data. *Anal Chem* **89**, 1063-1067

41. Le Cao, K. A., Gonzalez, I., and Dejean, S. (2009) integrOmics: an R package to unravel relationships between two omics datasets. *Bioinformatics* **25**, 2855-2856

42. Gonzalez, I., Cao, K. A., Davis, M. J., and Dejean, S. (2012) Visualising associations between paired 'omics' data sets. *BioData Min* **5**, 19

43. Subramanian, A., Tamayo, P., Mootha, V. K., Mukherjee, S., Ebert, B. L., Gillette, M. A., Paulovich, A., Pomeroy, S. L., Golub, T. R., Lander, E. S., and Mesirov, J. P. (2005) Gene set enrichment analysis: a knowledge-based approach for interpreting genome-wide expression profiles. *Proc Natl Acad Sci U S A* **102**, 15545-15550

44. Thijssen, S., Maringwa, J., Faes, C., Lambrichts, I., and Van Kerkhove, E. (2007) Chronic exposure of mice to environmentally relevant, low doses of cadmium leads to early renal damage, not predicted by blood or urine cadmium levels. *Toxicology* **229**, 145-156

45. Califano, D., Furuya, Y., Roberts, S., Avram, D., McKenzie, A. N. J., and Metzger, D. W. (2018) IFN-gamma increases susceptibility to influenza A infection through suppression of group II innate lymphoid cells. *Mucosal Immunol* **11**, 209-219

46. Go, Y. M., Sutliff, R. L., Chandler, J. D., Khalidur, R., Kang, B. Y., Anania, F. A., Orr, M., Hao, L., Fowler, B. A., and Jones, D. P. (2015) Low-Dose Cadmium Causes Metabolic and Genetic Dysregulation Associated With Fatty Liver Disease in Mice. *Toxicological sciences* **147**, 524-534

47. Li, S., Park, Y., Duraisingham, S., Strobel, F. H., Khan, N., Soltow, Q. A., Jones, D. P., and Pulendran, B. (2013) Predicting network activity from high throughput metabolomics. *PLoS Comput Biol* **9**, e1003123

48. Moya, M., Bautista, E. G., Velazquez-Gonzalez, A., Vazquez-Gutierrez, F., Tzintzun, G., Garcia-Arreola, M. E., Castillejos, M., and Hernandez, A. (2013) Potentially-toxic and essential elements profile of AH1N1 patients in Mexico City. *Sci Rep* **3**, 1284

49. Chistiakov, D. A., Sobenin, I. A., Orekhov, A. N., and Bobryshev, Y. V. (2015) Myeloid dendritic cells: Development, functions, and role in atherosclerotic inflammation. *Immunobiology* **220**, 833-844

50. Hastings, K. T., and Cresswell, P. (2011) Disulfide reduction in the endocytic pathway: immunological functions of gamma-interferon-inducible lysosomal thiol reductase. *Antioxid Redox Signal* **15**, 657-668

51. Phan, U. T., Lackman, R. L., and Cresswell, P. (2002) Role of the C-terminal propeptide in the activity and maturation of gamma -interferon-inducible lysosomal thiol reductase (GILT). *Proc Natl Acad Sci U S A* **99**, 12298-12303

52. Rezaee, F., and Georas, S. N. (2014) Breaking barriers. New insights into airway epithelial barrier function in health and disease. *Am J Respir Cell Mol Biol* **50**, 857-869

53. Hu, X., Fernandes, J., Jones, D. P., and Go, Y. M. (2017) Cadmium stimulates myofibroblast differentiation and mouse lung fibrosis. *Toxicology* **383**, 50-56

54. Desouza, M., Gunning, P. W., and Stehn, J. R. (2012) The actin cytoskeleton as a sensor and mediator of apoptosis. *Bioarchitecture* **2**, 75-87

55. Nemery, B. (1990) Metal toxicity and the respiratory tract. *Eur Respir J* **3**, 202-219

56. Choi, S. M., Jeong, Y. J., Park, J. S., Kang, H. J., Lee, Y. J., Park, S. S., Lim, H. J., Chung, H. S., and Lee, C. H. (2014) The impact of lifestyle behaviors on the acquisition of pandemic (H1N1) influenza infection: a case-control study. *Yonsei Med J* **55**, 422-427

57. Fiore, A. E., Fry, A., Shay, D., Gubareva, L., Bresee, J. S., and Uyeki, T. M. (2011) Antiviral agents for the treatment and chemoprophylaxis of influenza --- recommendations of the Advisory Committee on Immunization Practices (ACIP). *MMWR Recomm Rep* **60**, 1-24

58. Lee, B. K., and Kim, Y. (2016) Association of Blood Cadmium Level with Metabolic Syndrome After Adjustment for Confounding by Serum Ferritin and Other Factors: 2008-

2012 Korean National Health and Nutrition Examination Survey. *Biol Trace Elem Res* **171**, 6-16

59. Olsson, I. M., Bensryd, I., Lundh, T., Ottosson, H., Skerfving, S., and Oskarsson, A. (2002) Cadmium in blood and urine--impact of sex, age, dietary intake, iron status, and former smoking--association of renal effects. *Environ Health Perspect* **110**, 1185-1190
60. Ramsey, C. D., and Kumar, A. (2013) Influenza and endemic viral pneumonia. *Crit Care Clin* **29**, 1069-1086
61. Larsson, S. C., and Wolk, A. (2016) Urinary cadmium and mortality from all causes, cancer and cardiovascular disease in the general population: systematic review and meta-analysis of cohort studies. *Int J Epidemiol* **45**, 782-791
62. Haddam, N., Samira, S., Dumont, X., Taleb, A., Lison, D., Haufroid, V., and Bernard, A. (2011) Confounders in the assessment of the renal effects associated with low-level urinary cadmium: an analysis in industrial workers. *Environ Health* **10**, 37
63. Wang, Y., De Keulenaer, G. W., and Lee, R. T. (2002) Vitamin D(3)-up-regulated protein-1 is a stress-responsive gene that regulates cardiomyocyte viability through interaction with thioredoxin. *J Biol Chem* **277**, 26496-26500
64. Yamawaki, H., Pan, S., Lee, R. T., and Berk, B. C. (2005) Fluid shear stress inhibits vascular inflammation by decreasing thioredoxin-interacting protein in endothelial cells. *J Clin Invest* **115**, 733-738
65. Pader, I., Sengupta, R., Cebula, M., Xu, J., Lundberg, J. O., Holmgren, A., Johansson, K., and Arner, E. S. (2014) Thioredoxin-related protein of 14 kDa is an efficient L-cystine reductase and S-denitrosylase. *Proc Natl Acad Sci U S A* **111**, 6964-6969
66. Gocmen, C., Kumcu, E. K., Secilmis, A., Ucar, P., Dikmen, A., and Baysal, F. (2000) Restorative effects of zinc and selenium on nitrergic relaxations impaired by cadmium in the mouse corpus cavernosum. *Toxicol Lett* **111**, 229-234

Figure Legends

Figure 1. Cd worsened pathology of H1N1 infection. Mice were given ad libitum drinking water without or with $CdCl_2$ (1 mg/L) for 16 weeks; ten days prior to completion, mice in both groups were given one intranasal dose of either sterile saline (Ctl, Cd) or H1N1 influenza virus (H1N1, Cd+H1N1). Lung tissue was collected and formalin-fixed upon sacrifice at Day 10 after infection. Representative images of hematoxylin and eosin-stained sections of lung tissue are shown for each group (scale bar: 100 µm). Bar plots show % (mean ± SEM) of control (ctl) (n = 4-5 mice per group). *$p < 0.05$ compared to Ctl by Student's t-test. #$p < 0.05$ compared to H1N1 by Student's t-test.

Figure 2. Cd increased lung immune cell response to H1N1 infection. Cells were isolated from lung tissue homogenates, labeled with appropriate antibodies for (A) neutrophils (PMNs), (B) monocytes, (C) $CD11b^+$ dendritic cells (DCs), (D) $CD103^+$ DCs, (E) plasmacytoid DCs (pDCs), (F) $CD4^+$ T cells, (G) $CD8^+$ T cells and quantified by flow cytometry. Bar plots show mean ± SEM of cell counts (n = 11-13, except for $CD4^+$ and $CD8^+$ T cells, n = 7-8). *$p < 0.05$ compared to Ctl, #$p < 0.05$ compared to H1N1 by one-way ANOVA with Holm-Sidak's post-test.

Figure 3. Cd promotes mouse lung myeloid cell responses to H1N1 infection. Inflammatory lung tissue cell counts (7 cell types, **Fig. 2**), leading edge gene intensities (293 leading edge genes selected by GSEA, **Supplemental Table 2**;) and lung tissue metabolites measured by untargeted LC-MS (total of 2956 metabolic features, **Supplemental Table 1**) were correlated using sparse PLS regression implemented by xMWAS (n = 5/group). (A) Networks were constructed of variables with inter-dataset absolute association score >0.88 at $p < 0.05$ (n = 5) for

H1N1 or Cd+H1N1 groups. Symbols depict metabolic features (orange rectangle), gene transcripts (green circle) or cell counts (blue triangle), and lines indicate relationship between symbols (red, positive correlation; blue, negative correlation). The blue triangles have been enlarged for easier viewing. Abbreviations for cells are as follows: Monocytes, 'Mono'; neutrophils, 'PMN'; $CD11b^+$ dendritic cells, '$CD11b^+$ DC'; $CD103^+$ dendritic cells, '$CD103^+$ DC'; plasmacytoid dendritic cells, 'pDC'; CD4 T lymphocytes, '$CD4^+$'; and CD8 T lymphocytes, '$CD8^+$'. Note, $CD103^+$ DC is not found in the Cd+H1N1 network. (B) The absolute value of difference in eigenvector centrality (Delta Centrality) of each immune cell type was contrasted between the networks of Cd+H1N1 and H1N1 networks. Pearson's correlation (r) was analyzed for the abundance of lung IFN-γ protein and lung monocytes (**C**), $CD11b^+$ DCs (**D**) and neutrophils (E). Open circles, H1N1 alone; closed circles, Cd+H1N1. The resulting statistics of correlation (r) and significance (p) were as follows: **C**, monocytes (Cd+H1N1, r = 0.97, $p = 3\text{x}10^{-7}$; H1N1, r = 0.21, p = 0.49); **D**, $CD11b^+$ DCs (Cd+H1N1, r = 0.92, $p = 2\text{x}10^{-5}$; H1N1, r = -0.05, p = 0.86); **E**, neutrophils (Cd+H1N1, r = 0.89, $p = 9\text{x}10^{-5}$; H1N1, r = 0.22, p = 0.48). n = 12-13.

Figure 4. Cd potentiation of immune response to H1N1 infection through widespread effects of low Cd exposure on inflammation, mitochondrial function and regulation of immune cell populations through IFN-γ. (**A**) Percentage of gene sets represented in the 83 leading edge genes (**Supplemental Table 2**) with delta eigenvector centrality (absolute value), $|\text{Centrality}_{\text{Cd+H1N1}} - \text{Centrality}_{\text{H1N1}}|, \geq 0.1$ between Cd+H1N1 and H1N1 networks. (**B**) Metabolic pathway enrichment analysis was performed on 165 metabolic features with delta eigenvector centrality ≥

0.1 between networks of Cd+H1N1 and H1N1 using *mummichog*. The negative $\log_{10}$ of the pathway *p*-value is plotted as a bar graph for each significant pathway ($p < 0.05$, at least 3 metabolite matches in pathway).

Table 1. Cd increases pro-inflammatory gene enrichment in response to H1N1 challenge.

Gene Sets		**Enrichment**		
Name	Number of Genes	*H1N1 vs. Ctl*	*Cd+H1N1 vs. Ctl*	*Cd+H1N1 vs. H1N1*
Allograft rejection	189	3.02	3.21	2.31
Complement	181	2.36	2.56	1.73
Inflammatory response	199	2.61	2.75	1.84
Interferon-α response	89	2.79	2.88	2.04
Interferon-γ response	195	3.09	3.36	2.49
TNF-α signaling via NF-κB	196	2.60	2.82	2.06
Myogenesis	195	NA	-1.66	-2.14

Gene set normalized enrichment scores that are statistically significant comparing Cd+H1N1 and H1N1 ($p < 0.05$ and FDR $q < 0.05$) are shown. Normalized enrichment scores compared to controls (also $p < 0.05$ and FDR $q < 0.05$) are shown for H1N1 alone or Cd+H1N1. Negative enrichment values indicate *lower* gene abundances compared to the reference group (Ctl or H1N1, indicated in the column header). NA, gene set enrichment did not pass significance testing threshold.

Figure 1

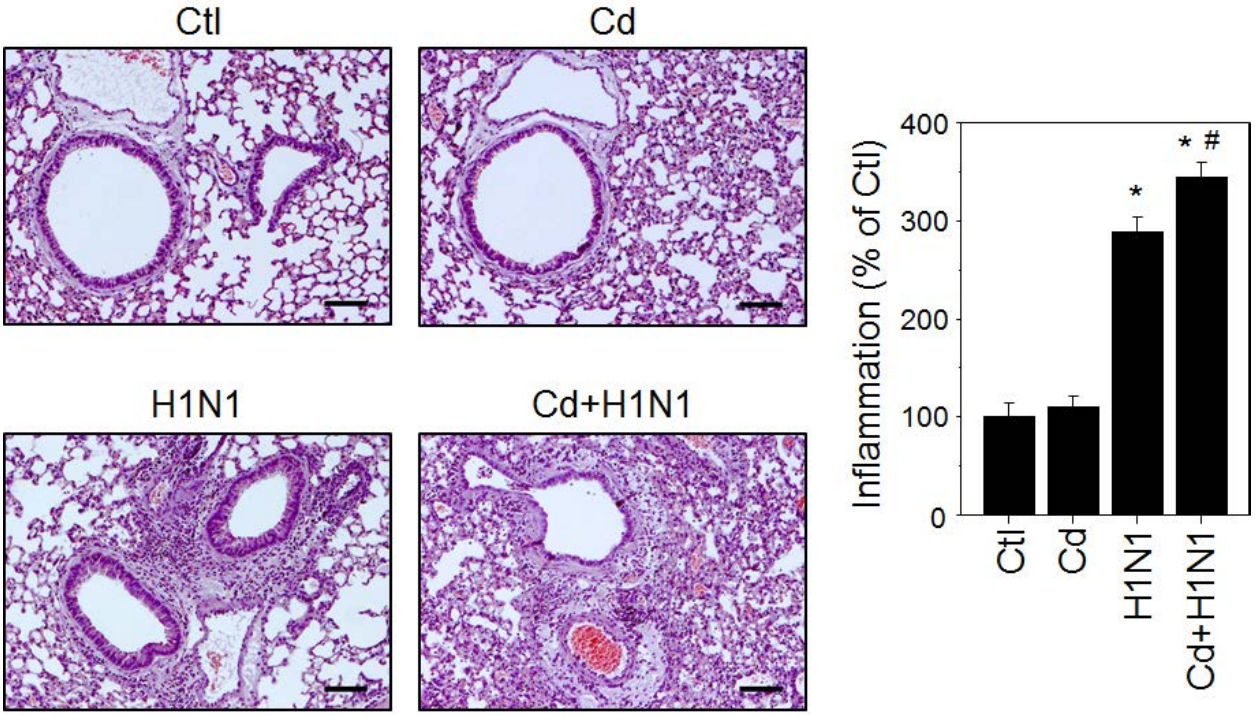

Figure 2

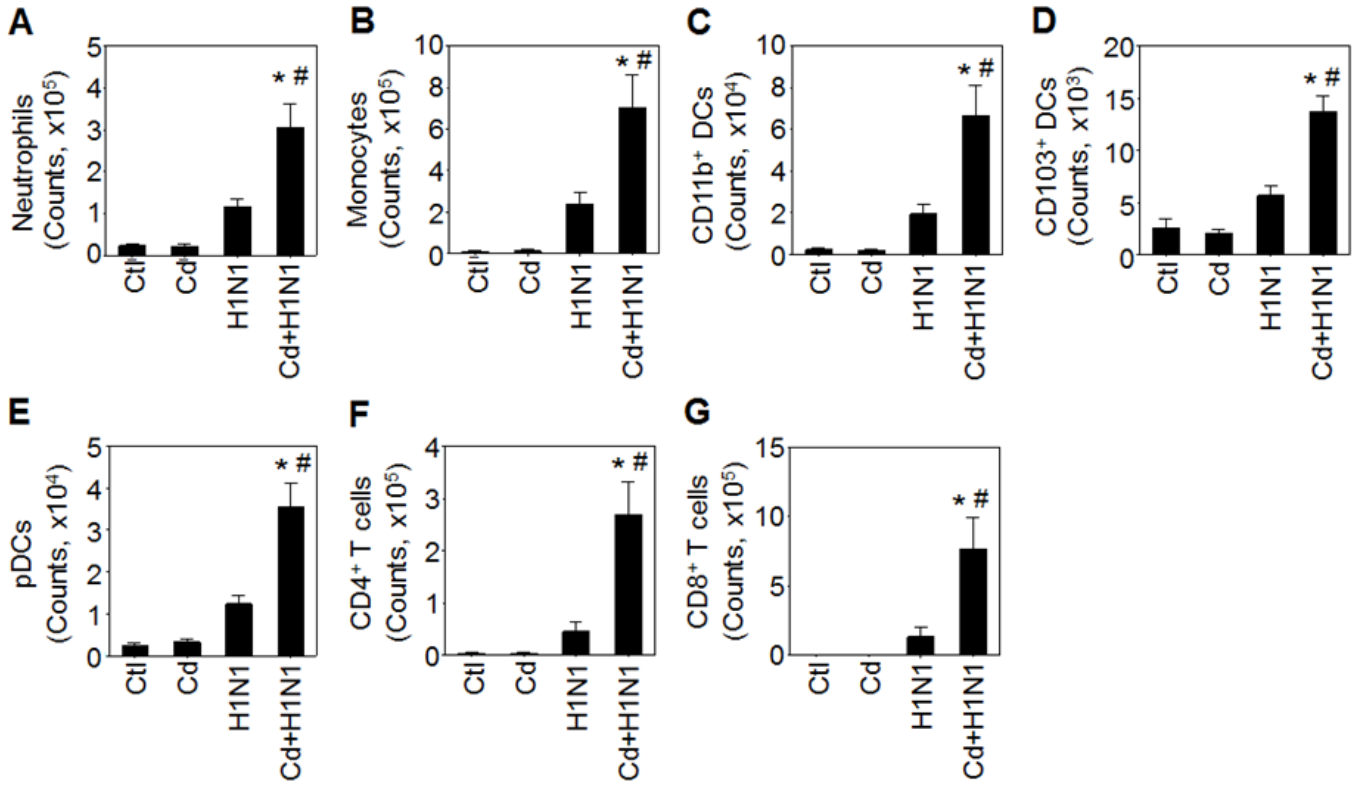

Figure 3

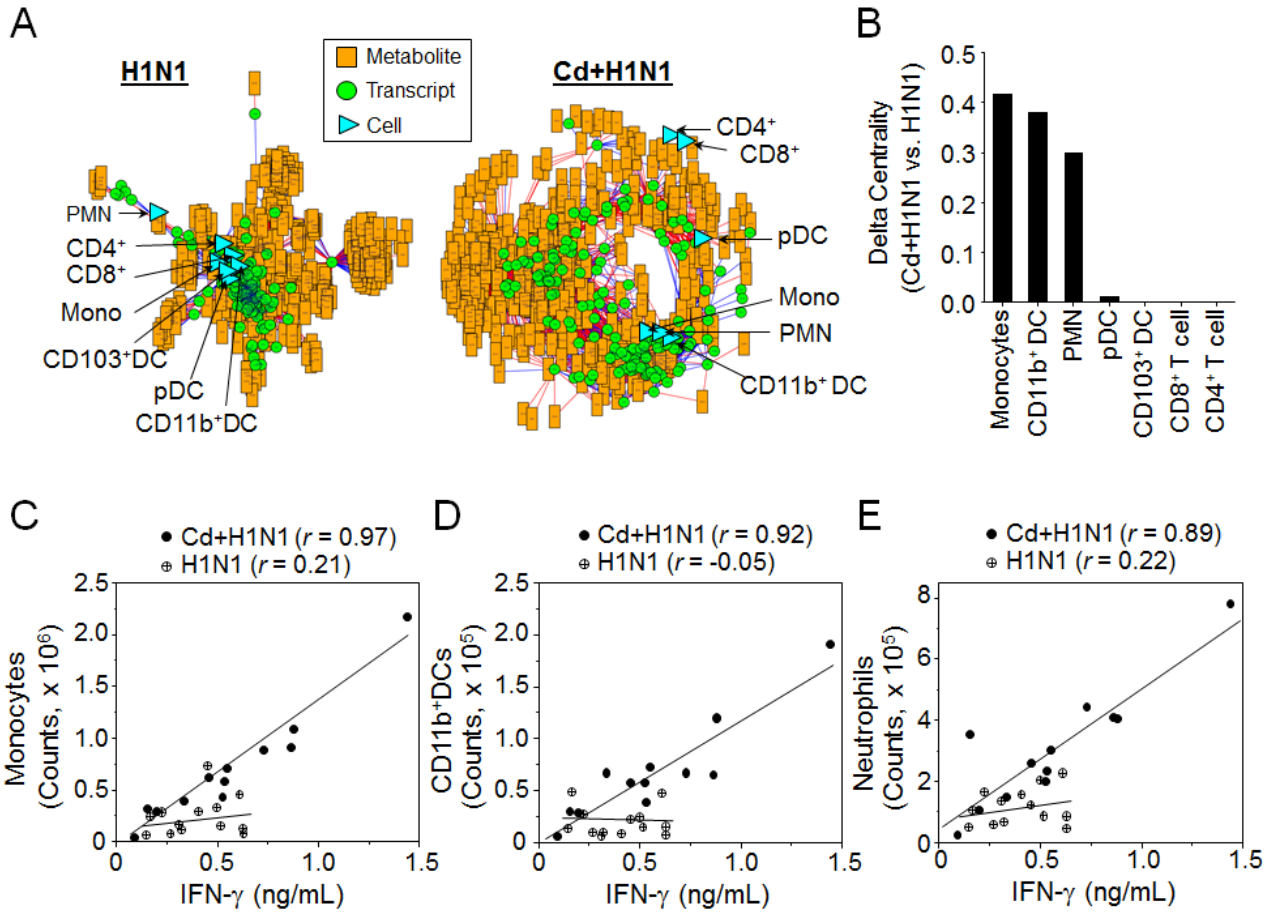

Figure 4